Journal of Fluorine Chemistry 240 (2020) 109665

Contents lists available at ScienceDirect

Journal of Fluorine Chemistry

journal homepage: www.elsevier.com/locate/fluor

Influence of Fluorination on Energetic Parameters of Silole, Phosphole, Thiophene, Oligomers of Silole and Related Acenes

Nguyen Ngoc Tri [a], Yohannes Mulugeta Hailu [b], Long Van Duong [c], Minh Tho Nguyen [c,d,*]

[a] Department of Chemistry, Faculty of Natural Sciences, Quy Nhon University, Quy Nhon, Viet Nam
[b] Department of Chemical Engineering, National Taiwan University of Science and Technology, Taipei, Taiwan
[c] Institute for Computational Science and Technology (ICST), Ho Chi Minh City, Viet Nam
[d] Department of Chemistry, KU Leuven, B-3001 Leuven, Belgium

ARTICLE INFO

Keywords:
Fluorination effects
Five-membered rings
Acenes
Silole oligomers
Energetic Parameters

ABSTRACT

The effects of fluorination on the energetic and thermochemical properties of a series of five-membered rings such as silole, phosphole and thiophene, and oligomers of silole and acenes were evaluated using density functional theory computations. Computed results indicate that substitution by fluorine atoms induces an increase of ionization energy and electron affinity and a decrease of proton affinity and HOMO-LUMO gap. For five-membered rings, fluorination effects are more significant on phosphole and silole as compared to those on thiophene. Changes in energetic properties of the oligomers of silole and acenes follow non-linear curves with increasing monomeric ring numbers. Effects of fluorination on energetic properties of the five-membered rings and oligomers are decreasing in the sequence of P-H > Si-H > C-H bonds. Replacement of H by F atom affects more strongly at Si-H bond than at C-H bond of siloles. Perfluorination of silole oligomers leads to derivatives with large electron affinity (> 4 eV). The anisotropy of induced current density (ACID) plots point out that fluorine replacement largely affects the electron delocalization at the C-C peripheral bonds in oligomers of silole and acenes. The silole unit emerges as a promising five-membered heterocycle to be used to tune up properties of oligomers.

1. Introduction

Heterocyclic compounds including the five-membered rings such as borole, pyrrole, furan, thiophene, and the six-membered rings such as pyridine and their fused benzene derivatives have constantly attracted attention and widely been investigated [1–6]. As important components of living organisms, heterocycles are involved in several life processes [7]. In fact, more than 90% of new drugs distributed in recent years contain heterocycles [8,9]. These cyclic compounds show peculiar properties including their electronic structure, stability and reactivity as compared to those of benzene and some other fused aromatic hydrocarbons. Discovery of their new applications can be promoted if deeper insights into the nature of their characteristics can be revealed. For such a purpose, quantum chemical computations have been proven to be an efficient and convenient approach for predicting electronic structure and properties of heterocyclic compounds [10–12].

As for a promising merit of heterocycles, let us mention their electron accepting ability. Acenes have long been known for their abilities, among others, to receive electrons [13,14]. Their behavior is similar to that of fullerenes that form ionic compounds with electron donors such as alkali metals [15], or of polycyano olefins that are known to accept electrons from a variety of donors [13,16]. Recently, siloles that are five-membered cycles containing a Si group, have been demonstrated to possess a high capacity for accepting electron. In this context it is of interest to have a systematic comparison of properties of this type of heterocycles to those of the better known acenes.

Of the five-membered analogues of thiophenes, siloles emerge as one effective candidate for electron transport materials [17,18]. In fact, siloles have fast electron mobility and high stability in the air and are also efficient emitters with very high brightness and external quantum yield [19]. The aggregation-induced emission phenomenon has been observed in some silole derivatives, in which the electroluminescence (EL) performance increases dramatically, going from solution to thin film [20,21]. Due to such significant properties, siloles and their derivatives have been proposed for use as light-emitting layers in EL devices [22,23]. Earlier theoretical investigations have already been

* Corresponding author.
E-mail address: minh.nguyen@kuleuven.be (M.T. Nguyen).

https://doi.org/10.1016/j.jfluchem.2020.109665
Received 24 May 2020; Received in revised form 8 October 2020; Accepted 9 October 2020
Available online 15 October 2020
0022-1139/© 2020 Elsevier B.V. All rights reserved.

conducted on silole monomers with different substituents, and oligo (2, 5-silole)s [24,25]. Structure-property relationships of silole monomers bearing symmetric electron donor–acceptors on 2-, 5-positions and different substituents on silicon atom were recently experimentally and theoretically studied [26]. Recent study of Boydston's silole systems revealed many new and interesting features that could be used for further experimental findings [27]. Similar to the well-known thiophenes, oligomers and polymers made from silole units are characterized with small band gaps [28,29].

Another avenue to tune up the properties of a class of compounds is through the conventional substituent effects. Fluorine substitution on the aromatic compounds is known to strongly influence some of their thermochemical parameters such as the electron affinity, charge mobility, excitation energy and absorption spectra [13,30–34]. Further, the presence of perfluorobenzene units in a chain of thiophene oligomers can also substantially modify their semiconducting behaviour [35]. Overall, fluorinated derivatives induce several beneficial effects on electronic properties. Although perfluoro-cyclic molecules are also regarded as another class of electron attracting compounds [36,37], they have not so far attracted much attention. A rational for the effects of fluorination on the properties of five-membered rings and their oligomers is not available yet.

In this context, we set out to explore the prospects for perfluoro-heterocyclic compounds to serve as electron acceptors using quantum chemical methods, for which suitable experiments to evaluate their EA values are not readily available [38]. Herein, we investigate the systematic influences of fluorination on several characteristic properties of five-membered analogues including silole, phosphole and thiophene and oligomers of silole. The latter properties are compared to those of acenes having comparable sizes. More specifically, frontier orbital energy gap, electron affinity, ionization potential, hardness and binding energies of five-membered rings, oligomers and acenes and their perfluoro-derivatives are explored.

2. Computational Methods

All electronic structure calculations are performed using the Gaussian 09 suite of programs [39]. Geometries of different five-membered rings and oligomers of silole and acenes are optimized using density functional theory (DFT) methods with the popular hybrid B3LYP functional in conjunction with the polarization 6-31 G(d,p) (for five-membered rings) and 6-311++G(d,p) (for oligomers of silole and acenes) basis sets [28,29]. Harmonic vibrational frequencies for gas phase structures are also computed to confirm the minima on the potential energy surfaces at the same level. Energetic properties that are calculated and analyzed, include the LUMO and HOMO energy levels, first excitation energy and thereby frontier orbital energy gap (E_g), electron affinity (EA), ionization energy (IE), proton affinity (PA) using single-point electronic energy at a higher level B3LYP/6-311++G(2df, 2p) with geometries taken from optimizations. Frontier orbital energies are taken from closed-shell geometries, and the unrestricted formalism (UB3LYP) is used for electronic open-shell structures.

The hardness (η) of compounds and homolytic bond dissociation energies (BDE) of C-H, Si-H, Si-F bonds in molecules are computed at the same level as the EA. All the parameters mentioned are calculated following the conventional protocols [40–43] including:

$$EA = E(M) - (EM\text{-}) + \Delta ZPE$$

$$IE = E(M+) - E(M) + \Delta ZPE$$

$$PA = -\Delta H = E(M\text{-}H+) - E(M) - E(H+) + \Delta ZPE + \Delta TCE$$

$$\eta = IE - EA;\ BDE = E(M\text{-}H) - E(M) - E(H) + \Delta ZPE$$

in which M is denoted for considered systems, E single-point total energy obtained at the B3LYP/6-311++G(2df,2p) level, ZPE zero-point energy correction and TCH being thermal correction to enthalpy calculated at B3LYP/6-31 G(d,p) for five membered rings or B3LYP/6-311++G(d,p) for oligomers of silole and acenes. Let us note that for the sake of consistency when plotting correlations between energetic parameters, the EA, EA and PA are all given in eV.

3. Results and Discussion

3.1. Structure and electronic properties of five-membered ring systems

The optimized structures of the five-membered cyclic systems are obtained at the B3LYP/6-31 G(d,p) level and shown in Fig. 1. F-derivatives are denoted by **Y-nFi** with Y = Si, P, S; n = 1-6; i: sites of H atoms replaced by F. For example, **Y-1 Fa**, **Y-1 Fb**, **Y-1 Fc** correspond to 1 F-derivatives in which a H atom is replaced at the 1, 2, 3 sites of a ring; **Y-2 Fa**, **Y-2 Fb**, **Y-2 Fc** are 2 F-derivatives with two H atoms replaced at (1,1), (1,2), (1,3) sites, respectively; **Y-3 Fa**, **Y-3 Fb**, **Y-3 Fc** are 3 F-derivatives with three H atoms substituted at (1,1,2), (1,1,3), (1,2,3) sites, respectively. All Cartesian coordinates of the optimized structures and their energy values are tabulated in Tables S1, S2 and S3 of the Supplementary Information file (Sx stands for a Table or Figure given in the SI file). Some parameters of optimized geometries for selected five-membered rings are shown in Table S4 (SI file). The point groups obtained for both parent and perfluoro substituted derivatives of silole, phosphole and thiophene are C_{2v}, C_s and C_{2v}, respectively. High symmetry point groups are found in some 2 F, 4 F-derivatives for silole and thiophene systems. Other derivatives mostly have lower symmetry such as C_s or C_1. As expected, replacements of H by F atoms in derivatives reduce symmetry point groups as compared to initial monomers. Besides, calculated results indicate that replacement of H by F atoms leads to small changes in the cyclic framework, either in bond lengths or bond angles in optimized structures of their derivatives, up to ~ 0.03 Å and 1–3°, respectively, in comparison to the non-substituted monomers (cf. Table S4, SI file).

Energy gaps (E_g^{TD}) and maximum absorption wavelengths (λ_{max}) are obtained using the TD-DFT method [44–47] with the same functional and basis set. The electron affinity (EA), proton affinity (PA) and ionization energy (IE) of the oligomers are also calculated and listed in Tables 1–3. Illustrations of variations of energetic values for F-derivatives are shown in Figures S1, S2 and S3 (SI file). Most end up in weak correlations, in part due to large variations of energetic values of derivatives. Different fluorinations at the sites in these five-membered rings lead to variations of their electronic properties. Some good correlations are however achieved for the changes in EAs of siloles, PA1 of phospholes and thiophenes with respect to the ring number N, and can be expressed as follows:

$$EA = 0.17 + 0.21\ N \text{ (silole)}$$

$$PA1 = 849.35 - 23.10\ N \text{ (phosphole)}$$

$$PA1 = 731.88 - 21.12\ N \text{ (thiophene) } (R^2 \approx 0.8).$$

Concerning the electron distribution, fluorination in these rings leads, as expected, to an increasing polarization of the C/Si/P-F bonds.

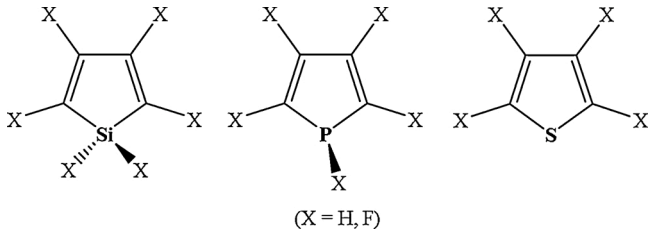

Fig. 1. Chemical structure of five-membered rings and their fluorinated derivatives.

Table 1
Calculated energetic parameters for silole and its F-derivatives (B3LYP/6-311++G(2df,2p)//B3LYP/6-31 G(d,p), IE, EA, PA, E_{gap}^{TD} in eV, λ in nm).

	IE	EA	PA1	PA2	PA3	PA4	PA5	HOMO	LUMO	E_{gap}^{TD}	λ_{max}
Silole	8.8	0.0	8.5	8.5	8.5			−6.3	−1.4	4.4	140
Si-1 Fa	8.8	0.6	8.4	8.4	8.4			−6.5	−1.8	4.1	146
Si-1 Fb	8.4	0.3	6.4	8.1	7.8	8.7	8.7	−6.1	−1.4	4.2	146
Si-1 Fc	8.7	0.3	8.6	8.6	6.9	7.0	8.1	−6.4	−1.5	4.4	145
Si-2 Fa	9.1	0.8	6.8	8.0	6.8			−6.8	−2.1	4.1	143
Si-2 Fb	8.7	0.8	6.8	8.0	7.5	8.5	8.5	−6.4	−1.9	3.9	149
Si-2 Fc	9.0	0.8	6.3	8.4	7.7	6.8	8.0	−6.7	−1.9	4.1	147
Si-2 Fd	8.5	0.5	8.4	8.2	7.2	6.8	8.4	−6.2	−1.6	4.1	147
Si-2 Fe	8.6	0.4	8.8	7.7	7.5	6.9	8.8	−6.3	−1.5	4.3	147
Si-2 Fg	8.3	0.4	6.9	8.3	7.6			−6.0	−1.5	4.0	152
Si-2 Fh	8.9	0.4	8.3	8.3	6.7			−6.6	−1.5	4.6	144
Si-3 Fa	8.9	1.0	6.6	7.7	7.3	6.5	8.3	−6.6	−2.1	3.9	147
Si-3 Fb	9.2	1.0	6.2	8.2	7.2	6.5	7.6	−6.9	−2.2	4.2	145
Si-3 Fc	8.8	0.9	6.6	8.0	7.0	7.0	8.2	−6.4	−2.1	3.8	146
Si-3 Fd	8.9	0.9	5.4	7.5	7.3	6.7	8.6	−6.6	−2.0	3.9	150
Si-3 Fe	8.6	0.9	6.9	8.0	7.3			−6.3	−2.0	3.6	154
Si-3 Fg	9.1	0.9	6.2	8.1	6.4			−6.8	−2.0	4.3	145
Si-3 Fh	8.7	0.5	8.5	7.9	7.0	6.7	8.5	−6.5	−1.6	4.3	146
Si-3 Fi	8.4	0.6	6.6	8.4	7.1	7.4	7.9	−6.2	−1.6	4.0	150
Si-4 Fa	9.0	1.1	6.5	7.8	6.8	6.3	7.9	−6.7	−2.3	3.8	147
Si-4 Fb	9.1	1.1	5.2	7.3	7.1	7.4	8.3	−6.8	−2.2	4.0	149
Si-4 Fc	8.8	1.1	6.8	7.8	7.1			−6.5	−2.2	3.7	151
Si-4 Fd	9.4	1.1	6.1	7.8	6.1			−7.1	−2.2	4.3	144
Si-4 Fe	9.0	1.0	6.3	7.6	6.9	6.4	8.3	−6.7	−2.1	4.0	146
Si-4 Fg	8.7	1.0	6.5	8.1	6.9	7.2	7.6	−6.4	−2.1	3.6	155
Si-4 Fh	8.6	0.7	6.7	8.1	7.1			−6.3	−1.7	4.1	148
Si-5 Fa	9.2	1.2	6.2	7.4	6.6	7.2	8.0	−6.9	−2.3	4.1	147
Si-5 Fb	9.0	1.2	6.4	7.9	6.7	7.0	7.4	−6.6	−2.3	3.7	151
Si-5 Fc	8.9	1.2	6.7	7.8	6.9			−6.6	−2.2	3.7	151
Si-6 F	9.1	1.3	6.6	7.6	6.6			−6.8	−2.4	3.8	149

Table 2
Calculated energetic parameters for phosphole and its F-derivatives (B3LYP/6-311++G(2df,2p)//B3LYP/6-31 G(d,p), IE, EA, PA, E_{gap}^{TD} in eV, λ in nm).

	IE	EA	PA1	PA2	PA3	PA4	PA5	HOMO	LUMO	E_{gap}^{TD}	λ_{max}
Phosphole	8.5	−0.1	8.8	8.7	8.2			−6.3	−1.0	4.8	149
P-1 Fa	8.8	0.9	8.7	8.5	7.9			−6.6	−1.9	3.9	145
P-1 Fb	8.5	0.1	8.4	8.2	8.0	7.9	8.7	−6.2	−1.1	4.5	141
P-1 Fc	8.7	0.1	8.6	8.7	7.5	8.0	8.3	−6.4	−1.2	4.7	149
P-2 Fb	8.7	1.0	8.4	8.2	7.6			−6.4	−2.1	3.6	172
P-2 Fc	9.0	1.0	8.6	8.5	7.2	7.6	8.2	−6.7	−2.1	3.9	165
P-2 Fd	8.6	0.3	8.2	8.0	7.4	7.6	8.5	−6.3	−1.3	4.4	143
P-2 Fe	8.6	0.2	8.2	7.5	7.7	7.1	8.7	−6.3	−1.2	4.6	144
P-2 Fg	8.4	0.3	8.1	8.1	7.8			−6.1	−1.2	4.4	143
P-2 Fh	9.0	0.2	8.4	8.3	7.3			−6.6	−1.3	4.9	145
P-3 Fc	8.9	1.2	8.2	7.9	7.0			−6.5	−2.2	3.5	139
P-3 Fd	8.9	1.2	8.2	8.2	7.3	6.7	8.5	−6.6	−2.2	3.7	170
P-3 Fe	8.7	1.2	8.0	7.9	7.4			−6.4	−2.2	3.4	139
P-3 Fg	9.2	1.1	8.4	8.2	6.9			−6.9	−2.1	4.0	143
P-3 Fh	8.8	0.4	8.0	7.7	7.1	6.9	8.4	−6.5	−1.3	4.6	146
P-3 Fi	8.5	0.4	7.9	8.2	7.2			−6.2	−1.3	4.3	144
P-4 Fe	9.1	1.3	8.0	7.6	6.9			−6.8	−2.3	3.7	170
P-4 Fg	8.8	1.4	7.8	8.1	6.9	7.2	7.6	−6.5	−2.4	3.4	139
P-4 Fh	8.7	0.6	7.7	8.0	7.0			−6.4	−1.4	4.4	145
P-5 F	9.0	1.5	7.6	8.0	6.9			−6.7	−2.5	3.4	170

Table 3
Energetic parameters for thiophene and its F-derivatives (B3LYP/6-311++G(2df,2p)//B3LYP/6-31 G(d,p), IE, EA, PA, E_{gap}^{TD} in eV, λ in nm).

	IE	EA	PA1	PA2	PA3	PA4	PA5	HOMO	LUMO	E_{gap}^{TD}	λ_{max}
Thiophene	8.7	1.0	7.6	8.5	8.1			−6.3	−0.2	5.9	129
S-1 Fb	8.8	0.7	7.2	7.8	7.9			−6.4	−0.5	5.7	130
S-1 Fc	8.6	0.5	7.6	8.6	7.6	8.1	8.4	−6.3	−0.3	5.4	131
S-2 Fd	8.7	0.2	7.1	8.1	7.5	7.7	8.4	−6.4	−0.5	5.2	138
S-2 Fe	8.8	0.2	7.2	7.7	7.9			−6.4	−0.5	5.3	157
S-2 Fg	8.6	0.1	7.1	8.1	7.9			−6.2	−0.3	4.9	134
S-2 Fh	9.1	0.5	7.2	8.2	7.2			−6.8	−0.6	5.8	150
S-3 Fh	9.0	0.1	7.0	7.8	7.3	7.0	8.3	−6.6	−0.7	5.2	139
S-3 Fi	8.7	0.2	6.9	8.2	7.4	7.7	7.9	−6.3	−0.5	4.7	140
S-4 F	8.9	0.4	6.7	8.0	7.2			−6.6	−0.7	4.7	141

The negative and positive charge densities are highly located at the F and C/Si/P atoms in these bonds, respectively.

As given in Tables 1–3, while substitution by F atoms in silole and phosphole rings tends to increase IE, EA values, an increase of IE and a decrease of EA are obtained for thiophene rings. As the number of fused rings increases, a stronger effect on energetic properties is observed. In particular, the IE ad EA values increase in the ordering from mono-fluoro to per-fluoro derivatives for silole, phosphole. Similarly, for thiophene systems, IE values increase and EA values decrease following to the sequence from 1 F to 4 F derivatives. Additionally, we consider the trends of substitution for each cyclic system. The IE values decrease in the ordering silole > thiophene > phosphole, and **Si-nFi** > **P-nFi** > **S-nFi** for F-derivatives. Also, the EA values decrease in the ordering of thiophene > silole > phosphole and **Si-nFi** > **P-nFi** > **S-nFi**.

Noticeably, the trends of IE, EA changes in silole, phosphole and thiophene are in agreement with those of the Si, P and S atoms, indicating the preference for attaching/removing one electron at the heteroatomic X sites in these five-membered rings. In addition, the changes of F-derivatives are mainly due to effects of F atoms and C/Si/P-F bonds, which can stabilize the structures by providing more extended electron delocalization. In general, influences of fluorination at the heteroatomic sites in these rings are specific for phosphole and silole.

For derivatives **1 Fb** and **1 Fc** in which one H atom at C-H bonds is replaced by one F atom (cf. Tables 1–3), the IE values change only marginally in the range of 0.1-0.4, 0.2 and 0.1 eV for silole, phosphole and thiophene, respectively. The EA values tend to increase by 0.3, 0.2 and 0.2-0.4 eV corresponding to silole, phosphole, and thiophene, respectively. Considering other 1 F-derivatives **Si-1 Fa** and **P-1 Fa** that contains Si/P-F bonds, energetic values carry a rise of 0.6 eV (EA) for silole, and 0.2 (IE), 0.9 eV (EA) for phosphole. Likewise, parameters in 4 F-derivatives in which H atoms at both C-H and Si/P-H bonds are substituted by F atoms, are altered in the range of 0.1-0.6 (IE), 1.0-1.1 (EA) eV for silole and of 0.3-0.5 (IE), 1.3-1.4 (EA) eV for phosphole. For derivatives **Y-4 Fh** without having Si/P-F bonds, the changes amount to 0.1, 0.2, 0.2 eV for IE, and 0.7, 0.7, 0.5 eV for EA in silole, phosphole, thiophene rings, respectively. Overall, fluorination effects are more important on the EA than on the IE, and increasing from the C-H to Si-H and finally to P-H bonds. The substituted rings having P-F bonds exhibit the largest EA values.

The possible protonation sites in silole, phosphole and thiophene are shown in Fig. 2. Accordingly, the most stable species of each form have resonance structures following conjugation effects. The PAs at sites in these rings tend to slightly reduce, *ca.* 0.0-0.9 eV in derivatives as compared to non-substituted monomers, and in going from derivatives 1 F to 4 F (thiophene), 5 F (phosphole) or 6 F (silole). A small increase is found in 1 F, 2 F and 3 F derivatives for silole, *ca.* 0.3 eV. Remarkably, the highest ability for protonation is achieved at C-H(F) sites (C2 or C5) while the lowest affinity is found at X sites for Si, S and C3 or C4 sites (C-F) for P. Most of strong and weak protonation processes are preferred in same derivative such as **Si-1 Fb**, **P-2 Fe**, **S-3 Fh** for each system.

Calculated frontier molecular orbital (FMO) energies and corresponding band gaps of closed-shell molecules are given in Tables 1–3 and their shapes are depicted in Figures S1, S2 and S3 (SI). Replacement of H by F atoms in initial monomers shows an increase in HOMO energies and a significant reduction in LUMO energies. In other words, the HOMOs are destabilized whereas the LUMOs are stabilized, and this leads to a decrease in FMO energy gaps. A consequence of such a change is a substantial decrease in the first electronic transition energies, expressed by the higher λ_{max} values in F-derivatives as compared to non-substituted species. This can be understood by the electron density overlap between p(MO) of fluorine atoms and π-electrons of C = C bonds in the five-membered rings, shown in Figures S4 and S5 (SI), leading to stronger electron delocalization for F-derivatives. Furthermore, the HOMO of thiophene is at a notably more negative energy level than phosphole or silole analogs due to their stronger π-electron conjugation involving the lone pair of sulfur atom (see Figure S4, SI). The LUMO of thiophene is also at a higher energy level than those of phosphole and silole. Compared to other five-membered rings, the LUMOs of silole are at significantly lower levels, which agrees well with earlier studies [3,7].

3.2. Acenes and perfluoro-acenes

3.2.1. Geometric structures of neutral, anion and cation species

Optimized structures for neutral and anion/cation states of acenes (n = 1-7) obtained at the B3LYP/6-311++G(d,p) level are shown in Fig. 3. Cartesian coordinates and single-point total energies of optimized structures are tabulated in Table S5 (SI). In fact, a D_{2h} group point is found for the groups of acenes from naphthalene to heptacene. When the acenes add/remove one electron to form anion/cation states, their symmetry can noticeably be kept with a high symmetry point-group (D_{6h}

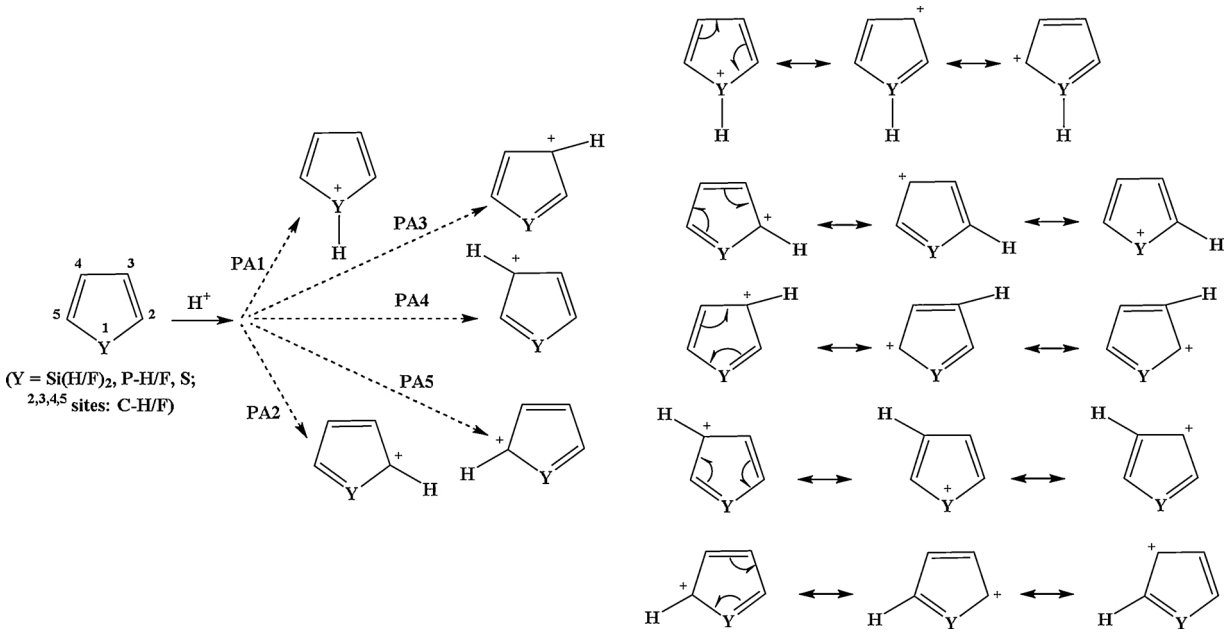

Fig. 2. Protonation sites in silole, phosphole, thiophene rings and their resonance structures.

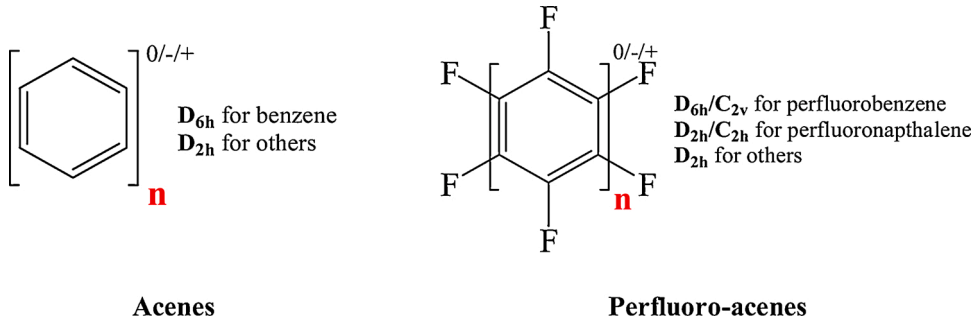

Fig. 3. Structures of acenes and perfluoro-acenes for neutral, anion and cation states, n = 1-7 (from one to seven rings, Optimized (U)B3LYP/6-311++G(d,p)).

for ions of benzene, D_{2h} for ions of larger acenes). This result indicates that the π-conjugated systems in these acenes are stable, well in line with a previous study [13].

The symmetry and stability of the fluorine substituted acenes are slightly altered when acenes with n = 3-7 in going from the neutral to ionic states. For perfluoro-benzene and perfluoro-naphthalene, the high D_{6h} and D_{2h} point groups are achieved for neutral species, while the lower C_{2v}/C_{2h} point groups are found for anion/cation states. For radical anions of benzene, naphthalene, and anthracene, the change in these structures is in an agreement with an earlier study [13]. Additionally, replacement of H by F atoms leads to a small change in molecular geometries. A large change in structural geometries is found for smaller rings such as benzene, naphthalene, whereas they remain almost unchanged for larger rings (n = 3-7). In these systems, the geometrical symmetries of the cationic and anionic states are markedly similar to the neutral derivatives of fluoro-acenes with n = 1-7. Thus, calculated results reveal that the conjugation in these acenes is quite strong, and only slightly perturbed upon one-electron removal or addition.

3.2.2. *Electronic properties of acenes and perfluoro-acenes*

For a deeper understanding of the changes of the orbital energy levels, we now investigate the shapes and energy levels of HOMOs and LUMOs for all acenes and perfluoro-acenes with n = 1-7. These results are analyzed and illustrated in Figs. 4 and S6 (SI) and listed in Table S7

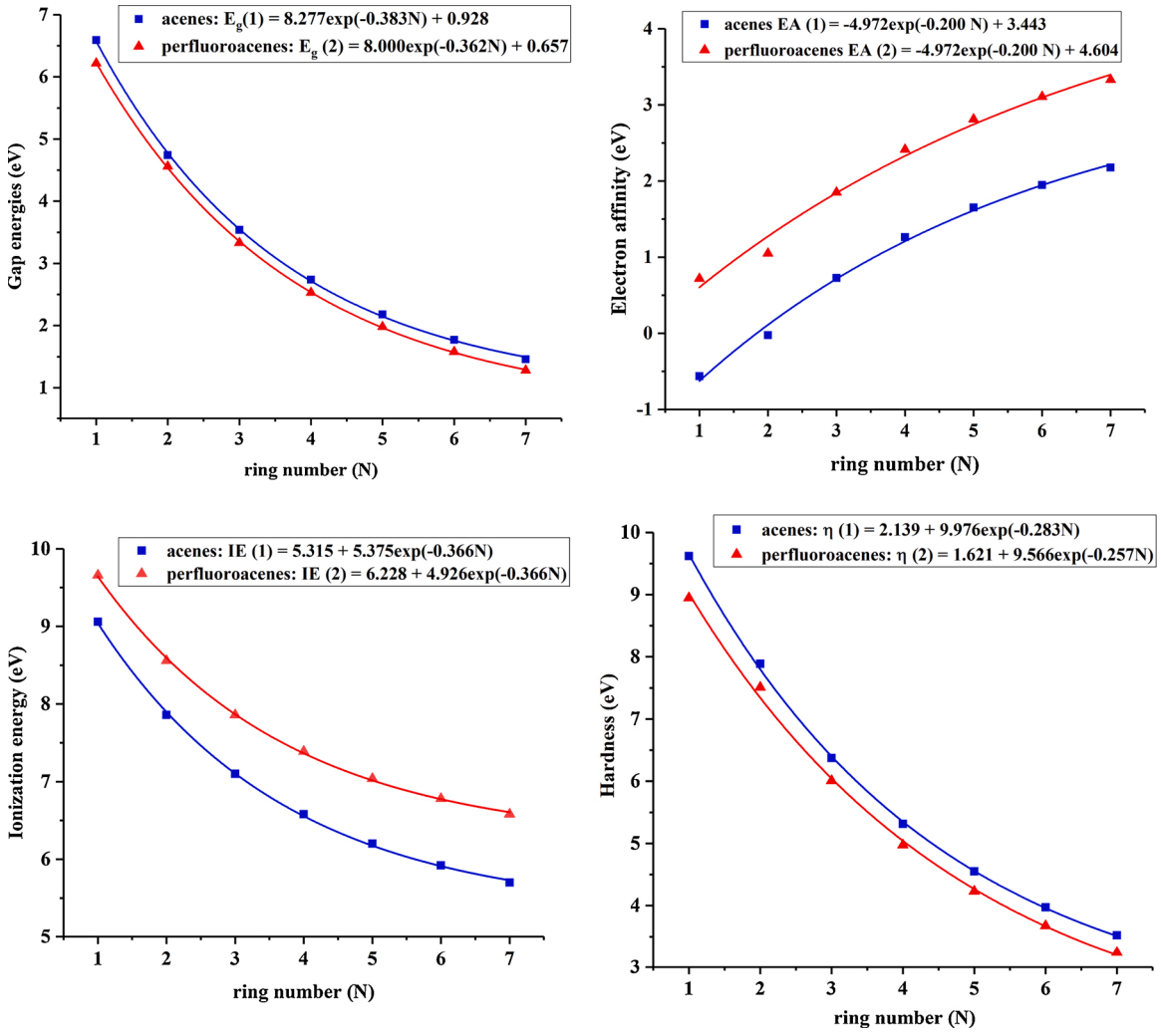

Fig. 4. Correlations of characteristic energetic parameters and ring number for acenes and perfluoro-acenes ($r^2 \approx 0.99$).

(SI). In general, delocalization in acenes and their F-derivatives is driven by electron density at π(C = C) bonding orbitals as displayed in HOMOs. Electron density is also manifested at their π*(C = C) and σ*(C-C) antibonding LUMOs. Replacement of H by F atoms again leads to a higher electron density and delocalization.

Frontier orbitals (FMO) are crucial for understanding reaction mechanism of organic molecules. A change in FMO shapes and levels leads to a change in reaction pathway and band gaps. Moreover, when one electron is removed from, or added to, FMOs lead to changes in structure. Figure S6 shows that the shapes of HOMOs/SOMOs and LUMOs at neutral and ionic states in acenes/perfluoro-acenes are slightly different from each other. This implies small changes in the structure and HOMO-LUMO gaps. A significant difference appears at n = 1 for the LUMOs of benzene and perfluoro-benzene. Hence, the high symmetry of LUMO of perfluoro-benzene brings in substantial changes to the anionic states.

The energy gap (E_g) of a molecule is also a key parameter for evaluating its electronic behaviour. Figure 4 illustrates the variations of E_g values as function of the number of benzene ring N in acenes/perfluoro-acenes. Table 4 summarizes these expressions obtained as in equations (1) and (2) for acenes and perfluoro-acenes, respectively. In comparison to acenes, formation of C-F bonds affects in reducing the energy gap by *ca.* 0.3 eV for all N sizes. Similarly, a good correlation between energy gaps and number of rings for perfluoro-acenes is observed. Substitutions by F atoms induce strong polarization of C-F bonds which can bring significant changes in the electronic structure and energy gaps of fluoro-derivatives in relative to acenes. Delocalization of electron densities in acenes is focused on benzene rings whereas in perfluoro-acenes, electron densities are delocalized at both benzene rings and C-F bonds (see Figure S6). Hence, the π-electron conjugation observed for F-derivatives is more expanded. The band gaps become smaller for fluoro-acenes, as the trend of reducing energy gap in larger fused ring systems for perfluoro-acenes achieves a higher correlation (Fig. 4).

Electron affinities (EAs) of acenes and perfluoro-acenes behave in a proportional relationship with the ring numbers N (cf. Fig. 4). EA values for both benzene and anthracene are calculated to be negative (cf. Table S8), implying that the corresponding anions are not stable with respect to electron detachment, in agreement with an earlier study [13]. The larger positive EAs in perfluoro-acenes are thus the result of a remarkable effect of perfluorination [13]. In perfluoro-acenes, the electron density is located at both ring π-electrons (center) and C-F bonds (F side). This effect is illustrated in Figure S6 (SI). The $C^{\delta+}$-$F^{\delta-}$ polarity due to the electronegativity of F atom, and the larger electron delocalization in LUMOs of perfluoro-acenes makes them more conveniently attracting one electron and stabilizing the resulting anion. Good curved correlations between EA values and benzene-ring number N emerge, as shown in Fig. 4, and the correlation expressions (3) for acenes and (4) for perfluoro-acenes are established as shown in Table 4.

Table 4
High curved correlation equations of energetic parameters and ring number (N) for investigated systems.

Acenes	$E_{g(1)}=8.277e^{-0.383N}+0.928$	(1)	$E_{g(2)}=8.000e^{-0.362N}+0.657$	(2)
	$EA_{(1)}=5.38e^{-0.366N}+5.32$	(3)	$EA_{(2)}=4.93e^{-0.366N}+6.23$	(4)
	$IE_{(1)}=-4.972e^{-0.200N}+3.443$	(5)	$IE_{(2)}=-4.972e^{-0.200N}+4.604$	(6)
	$\eta_{(1)}=2.139+9.976e^{-}_{0.283N}$	(7)	$\eta_{(2)}=1.621+9.566e^{-}_{0.257N}$	(8)
Oligomers of silole	$E_{g(1)}=4.714e^{-0.399N}+1.633$	(9)	$E_{g(2)}=4.833e^{-0.497N}+1.757$	(10)
	$E_{g(3)}=4.760e^{-0.433N}+1.527$	(11)	$E_{g(4)}=4.959e^{-0.550N}+1.601$	(12)
	$EA_{(1)}=-3.480e^{-0.337N}+2.707$	(13)	$EA_{(2)}=-3.163e^{-0.423N}+2.828$	(14)
	$EA_{(3)}=-4.709e^{-0.361N}+4.165$	(15)	$EA_{(4)}=-4.525e^{-0.454N}+4.272$	(16)
	$IE_{(1)}=4.045e^{-0.340N}+5.638$	(17)	$IE_{(2)}=3.869e^{-0.299N}+5.724$	(18)
	$IE_{(3)}=3.006e^{-0.236N}+6.728$	(19)	$IE_{(4)}=3.067e^{-0.289N}+6.753$	(20)
	$\eta_{(1)}=7.517e^{-0.339N}+2.935$	(21)	$\eta_{(2)}=6.949e^{-0.350N}+2.940$	(22)
	$\eta_{(3)}=7.731e^{-0.331N}+2.607$	(23)	$\eta_{(4)}=7.233e^{-0.358N}+2.631$	(24)

Other characteristic parameters including ionization energy (IE) and hardness (η) are also illustrated in Fig. 4 and listed in Table S9 (SI). In fact, IE values are again found to be correlated with the benzene-ring number N as expressed in equations (5) for acenes and (6) for perfluoro-acenes (cf. Table 4). The hardness is often regarded as an important parameter for evaluating the reaction capacity of a molecule [38]. Here, some correlations between both parameters, hardness and benzene-ring number N, are also found in equations (7) for acenes and (8) for perfluoro-acenes in Table 4. Hardness values of acenes are slightly larger than those of perfluoro-acenes, resulted from changes in their EAs and IEs. Replacement of H by F atoms leads to lower ionization ability and larger IEs with a constant of ~ 0.8 eV. Similarly, the hardness of acenes is larger than that of fluoro-derivatives, with a constant of ~ 0.2 eV. The changes of hardness values are followed by correlations as illustrated in Fig. 4.

Fluorination effect is equally observed in the binding energy of C-H bonds in acenes. The BDE(C-H) values in CH_4, C_6H_6 and C_6HF_5 are 426, 456 and 483 kJ.mol^{-1}, respectively. Indeed, larger binding energy for C-H bond is computed in C_6HF_5 as compared to C_6H_6 and CH_4 (cf. Table S10). Besides, these calculated BDE(C-H) values are reasonable with a slightly difference of 5-16 kJ.mol^{-1} as compared to experimental data [48].

To probe further the electron delocalization of acenes and their F-derivatives, some selected monomers are now examined using the anisotropy of their induced current density (ACID) [49,50]. The ACID map is an efficient method for evaluating the degree of electron delocalization of conjugated rings on the basis of the magnetic indicator. The ACID isosurfaces of benzene, heptacene and their perfluoro-derivatives are calculated at the standard value of 0.05 and the current density vectors are plotted in Fig. 5 onto these ACID isosurfaces. The current density vectors emphasized by ACID analysis indicate a strong diatropic ring current along peripheral C-C bonds, which agrees well with previous studies [49,50]. The critical isosurface values (CIVs) are known in previous report [51] and understood in ref. [50]. Accordingly, they are ACID values at delocalized critical points. A higher CIV implies a stronger delocalization of electron density. As displayed in Fig. 5, the CIVs for C-C peripheral bonds in benzene and perfluorobenzene amount to 0.09 and 0.06, respectively. Consistent with previous studies [49,50], the largest degree of delocalization of the C-C peripheral bonds belongs to the central three-ring anthracene system in heptacene and perfluoroheptacene which exhibit CIVs of 0.10-0.11 and 0.08-0.09, respectively. The weakest CIV degree is found at the terminal rings in heptacene and its F-derivative with CIVs of *ca.* 0.05 and 0.09, respectively. The CIVs for C-F bonds in F-benzene and F-heptacene correspond each to 0.07. Indeed, perfluorination in these acenes leads to a decrease of density at C-C bonds and an increase at C-F bonds. For larger species like heptacene, a stronger electron delocalization is attained in comparison to benzene.

3.3. Oligomers of silole and their F-derivatives

3.3.1. Geometries of neutral, anionic and cationic states

The oligomers are examined from one to seven units of silole ring and are designed with anti-fused rings when considering electronic properties. The F-derivatives are formed by replacement of H at sites by F atoms following three ways: i) at Si-H bonds (siloles Si-F), ii) at C-H bonds (siloles C-F) and iii) at both Si-H and C-H bonds (perfluoro-siloles), as given in Fig. 6. Cartesian coordinates and total energies of these optimized geometries are collected in Table S6 (SI).

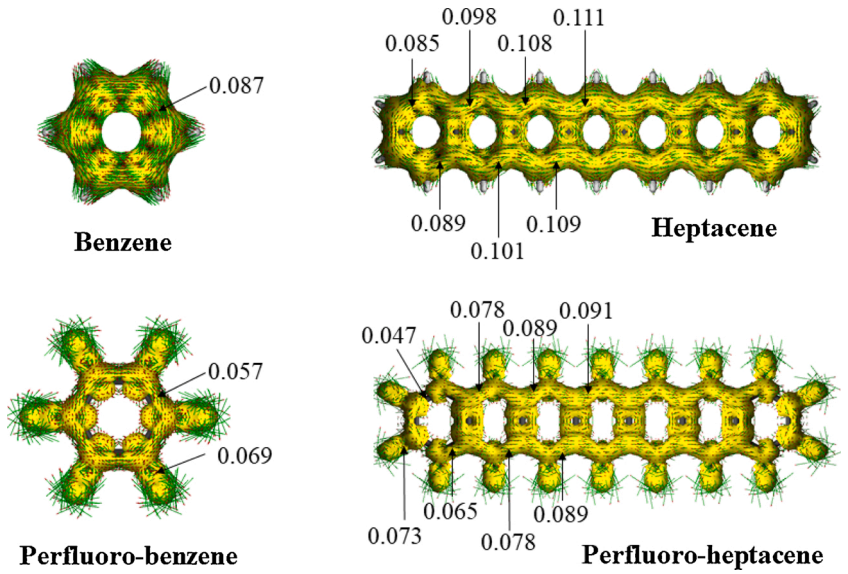

Fig. 5. ACID isosurfaces of benzene, heptacene and their F-derivatives (B3LYP).

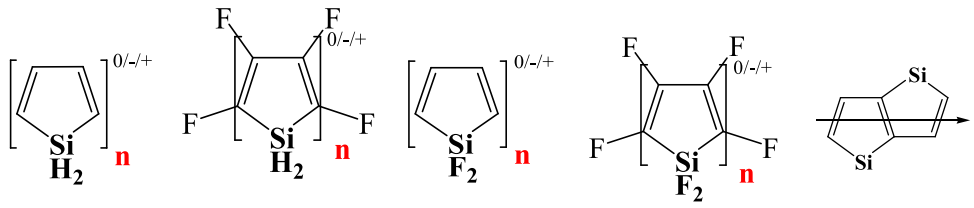

Symmetry point groups: C_{2v} *for n = 1,3,5,7;* C_{2h} *for n = 2,4,6* *Anti-fused rings*

Siloles **Siloles (C-F)** **Siloles (Si-F)** **Perfluoro-siloles**

Fig. 6. Structures of oligomers of silole and its F-derivatives with neutral, anion and cation states, n = 1-7 (optimized (U)B3LYP/6-311++G(d,p)).

Fig. 6 shows stable structures of siloles and perfluoro-siloles systems with symmetry point groups. F-substitutions induce only slight changes in geometrical structures. The point groups remain unchanged for F-substituted derivatives, also for anionic/cationic states. Hence, removal of one electron from, or addition of one electron to neutral silole or perfluoro-silole makes only minor changes in structures of anionic/cationic states. This can be viewed by π-electrons of C = C bonds in siloles indicated by HOMO, LUMO shapes (cf. Figure S7, SI).

3.3.2. *Electronic properties of oligomers of silole and their F-derivatives*

The shapes of HOMOs and LUMOs for oligomers of silole and perfluoro-silole are depicted in Figure S7 (SI), where the HOMOs are almost populated at C = C double bonds and a small addition at F atoms in silole (H/F) rings. For LUMOs, the electron density is located at anti-bonding orbitals of Si-C and C-C bonds. Table S11 (SI) shows that a F-substitution expectedly reduces the energy gaps considerably; the energy gap is significantly reduced as the number of fluorine atoms rises. Hence, the energy gap is lowered to a large extent for perfluoro-siloles. A good correlation ($r^2 \approx 0.99$) between the energy gaps and the number N of silole units can again be established (cf. Fig. 7).

Furthermore, changes in EA values for the oligomers of silole are substantial upon replacement of H by F for these oligomers going from n = 1 to 7. The effects of F-substitution to LUMO levels are significant and in agreement with results mentioned above for the monomers [13, 28]. When a H is substituted by an F, EA values become almost twice as large (see Table S12, SI).

Ionization energy (IE) and hardness (η) of oligomers of silole and perfluoro-silole compounds are also evaluated. These values are presented in Table S13 (SI) and illustrated in Fig. 7. F-substitution on the C atoms of π-conjugated ring leads to a decline of IE and hardness values as compared to non-substituted counterparts. Frontier orbital gaps, IE and η values drop along with an increasing number of fused rings of oligomers (see Fig. 7). Overall, highly curved correlations between energetic properties including E_g, EA, IE, η and N of oligomers of silole and their F-derivatives are again established and expressed in Table 4. The indices given as $(_{1,2,3,4})$ denote for siloles, siloles (C-F), siloles (Si-F) and perfluoro-siloles, respectively. The equations (9)-(12), (13)-(16), (17)-(20) and (21)-(24) equations are presented for correlations of E_g, EA, IE and η parameters with respect to the number of silole units N, respectively. Hence, changes in energetic properties are found in the ordering of siloles > siloles (C-F) > siloles (Si-F) > perfluoro-siloles in terms of E_g, IE, and η values. An increase of EA values is emphasized with the same ordering. In fact, a F-substitution of siloles at Si-H bonds yields stronger effects than that at C-H bonds (cf. Figure S7 and Tables S11, S12, S13), leading to significant changes in the trends of E_g, EA, IP and η.

Moreover, the effects are observed on bond dissociation energies (BDE) of Si-H/F bonds in siloles as presented in Table S14 (SI). Accordingly, the BDE (Si-H) values are reduced by 10-24 kJ.mol^{-1} in $C_4H_4SiH_2$ and $C_4F_4SiH_2$ as compared to that of SiH_4. The BDE(Si-F) values in $C_4H_4SiF_2$ and $C_4F_4SiF_2$ follow a rise by 27 kJ.mol^{-1} in comparison to that of SiF_4. Let us note that the calculated BDE values are consistent with available experimental data and other DFT study [48, 52]. Particularly, the calculated BDE(Si-H/F) values in SiH_4, $C_4H_4SiH_2$, $C_4F_4SiH_2$, SiF_4, $C_4H_4SiF_2$ and $C_4F_4SiF_2$ molecules correspond to 371,

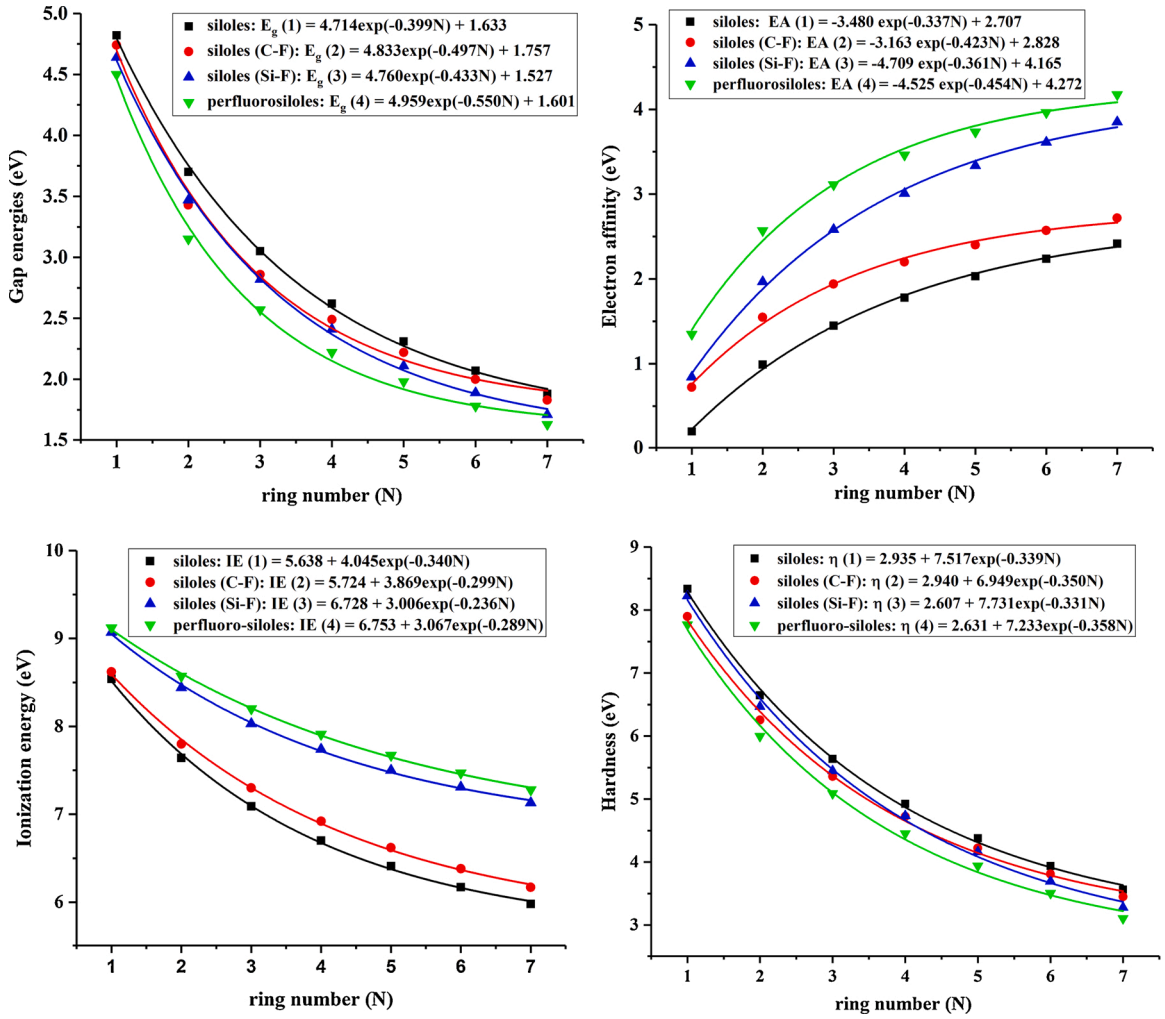

Fig. 7. Correlations of gap energies, electron affinity, ionization energy, hardness with ring number for oligomers of silole and their F-derivatives ($r^2 \approx 0.99$).

346, 362, 648, 621 and 621 kJ.mol^{-1} with deviation of 13 kJ.mol^{-1} (3%) for Si-H and 50 kJ.mol^{-1} (7%) for Si-F, as compared to available experimental data. As a consequence, the BDEs of Si-F bonds are only slightly different from each other, whereas large changes in BDE values are found for Si-H bonds in F-derivatives, in comparison to non-substituted molecules.

Some oligomers of silole and F-derivatives are now selected for an evaluation of electron delocalization by the ACID method [49,50], that is executed at standard isosurface values of 0.05. The corresponding plots are shown in Fig. 8. The ACID maps indicate strong diatropic ring currents in siloles and perfluoro-siloles. Similar to acenes, while the highest degree of electron delocalization is obtained at the ring center in both un- and F-substituted derivatives of siloles-7 (CIVs of ca. 0.09-0.10), the weakest one is found at terminal rings (CIVs ca. 0.07-0.10). In fact, a stronger delocalization is found in larger silole-7 rings with the higher CIVs as compared to silole-1 rings. The CIVs for Si-F bonds of 0.07 suggest that these bonds significantly contribute in affecting electron delocalization of the whole structures and electronic properties of silole rings. Overall, the influence of fluorination in oligomers of silole can be pointed out by a slight reduction of electron delocalization at C-C peripheral bonds and an enhancement at Si-F bonds.

4. Concluding Remarks

In the present theoretical study, we investigated the structural and thermochemical properties of the five-membered rings including siloles, phospholes and thiophenes, the oligomers of silole and acenes in the neutral, anionic and cationic states using density functional theory (DFT) calculations. The effects of fluorination on these molecules were explored upon examination of their thermochemical properties such as gap energy (E_g), electron affinity (EA), ionization energy (IE), proton affinity (PA), hardness (η), and bond dissociation energy (BDE).

For five-membered rings, the structural changes in F-derivatives are relatively small with respect to non-substituted monomer. Effects of replacement of H by F atoms in these molecules are identified with significant increases of IE, EA, and a decrease of PA, E_g values. In the related acene systems, while structures of anionic/cationic states are slightly distorted for n = 1, 2, they remain almost similar for n = 3–7 (with n being ring number) in comparison to their neutral states.

For oligomers of silole, the geometries of neutral and anion/cation states are noted with slight differences from each other for all n values. Fluorinated substitutions on silole rings lead to an increase in EA, IE and BDE, and a reduction in FMO energy gap and hardness values. Excellent correlations between energetic properties and number of silole/benzene units are identified for both series of silole and acene oligomer systems. More importantly, the cooperative effects of C-F and Si-F bonds, that replace C-H and Si-H bonds in acenes and siloles, lead to more significant changes of their characteristics. For siloles and phospholes, the effects exerted upon of replacement of H by F atoms at the Si/P-H bonds are more substantial than those at C-H bonds. Fluorination strongly affects the electron delocalization at C-C peripheral bonds in acenes and

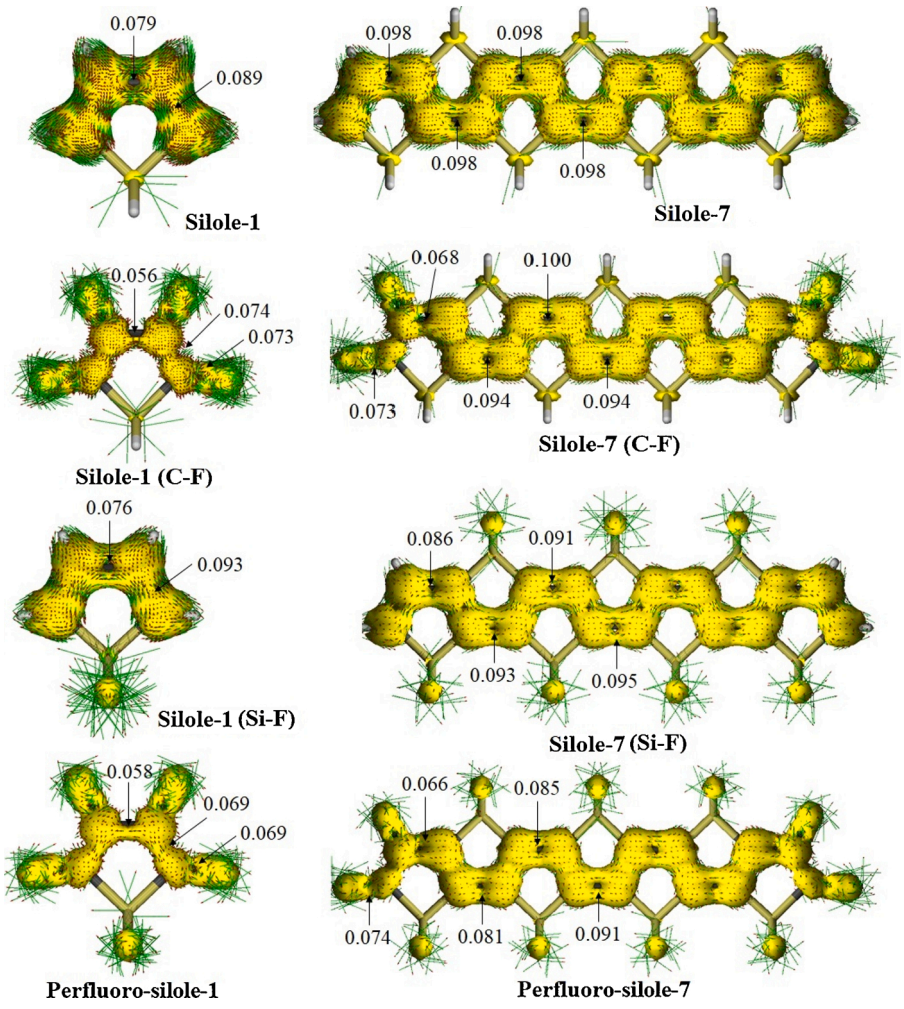

Fig. 8. ACID isosurfaces of oligomers of silole and some selected F-derivatives.

oligomers of silole, and also at the C-F/Si-F bonds of their F-derivatives. Remarkably, the largest EA is achieved in perfluoro-siloles whose EA value of ~4.2 eV is found for perfluoro-silole-7, more than 1.3 times as large as the EAs of perfluoro-heptacenes.

Declaration of Competing Interest

The authors report no declarations of interest.

Acknowledgements

Work at ICST was supported by Department of Science and Technology of Ho Chi Minh City, Vietnam, under Grant nr. 5/2018/Đ2/HĐ-KHCNTT (2019).

Appendix A. Supplementary data

Supplementary material related to this article can be found, in the online version, at doi:https://doi.org/10.1016/j.jfluchem.2020.109665.

References

[1] Y. Dai, T. Zhang, Y. Piao, X. Zhang, Y. Hu, L. Zhang, S. Jia, H. He, Computational study on fused five membered heterocyclic compounds containing tertiary oxygen, J. Mol. Struct. 1129 (2017) 98–104.
[2] H. Willsch, H. Clegg, B. Horsfield, A.M. Radke, H. Wilkes, Liquid chromatographic separation of sediment, rock, and coal extracts and crude oil into compound classes, Anal. Chem. 69 (1997) 4203–4209.
[3] Y.M. Hailu, M.P. Pham-Ho, M.T. Nguyen, J.C. Jiang, Silole and selenophene-based D-π-A dyes in dye-sensitized solar cells: Insights from optoelectronic and regeneration properties, Dyes Pigments 176 (2020), 108243.
[4] N.N. Tri, L.V. Duong, M.T. Nguyen, Optoelectronic properties of heptacene, its fluorinated derivatives and silole, thiophene analogues, Mater. Today Commun. 24 (2020), 1010542.
[5] F.V.S. Eric, A.R. Christopher, Advances in Heterocyclic Chemistry, Academic Press, 2016.
[6] J.H. Barnard, S. Yruegas, K. Huang, C.D. Martin, Ring Expansion Reactions of Anti-Aromatic Boroles: A Promising Synthetic Avenue to Unsaturated Boracycles, Chem. Commun. 52 (2016) 9985–9991.
[7] A.F. Pozharskiæi, A.R. Katritzky, A.T. Soldatenkov, Heterocycles in Life and Society: An Introduction to Heterocyclic Chemistry. Biochemistry and Applications, Wiley, 2011.
[8] E. Vitaku, D.T. Smith, J.T. Njardarson, Analysis of the structural diversity, substitution patterns, and frequency of nitrogen heterocycles among U.S. FDA approved pharmaceuticals, J. Med. Chem. 57 (2014) 10257–10274.
[9] M. Baumann, I.R. Baxendale, An overview of the synthetic routes to the best selling drugs containing 6-membered heterocycles, Beilstein J. Org. Chem. 9 (2013) 2265–2319.
[10] G. Vektariene, G. Vektaris, J. Svoboda, A theoretical approach to the nucleophilic behavior of benzofused thieno[3,2-b]furans using DFT and HF based reactivity descriptors, ARCIVOC 42 (2009) 311–329.
[11] J. Garcíacruz, J.M. Martínez-Magadan, A.R. Salcedo, F. Illas, Electronic structure properties of dibenzofurane and dibenzothiophene derivatives: implications on asphaltene formation, Energy Fuels 19 (2005) 998–1003.
[12] D. Valencia, T. Klimova, I. García-Cruz, Aromaticity of five- and six-membered heterocycles present in crude oils e an electronic description for hydrotreatment process, Fuel 100 (2012) 177–185.
[13] Y. Xie, H.F. Schaefer, F.A. Cotton, The radical anions and the electron affinities of perfluorinated benzene, naphthalene and anthracene, Chem. Commun. (2003) 102–103.

[14] J.C. Rienstra-Kiracofe, G.S. Tschumper, H.F. Schaefer, N. Sreela, G.B. Ellison, Atomic and Molecular Electron Affinities: Photoelectron Experiments and Theoretical Computations, Chem. Rev. 102 (2002) 231–282.
[15] I. Alkorta, I. Rogas, J. Elguero, Interaction of Anions with Perfluoro Aromatic Compounds, J. Am. Chem. Soc. 124 (2002) 8593–8598.
[16] F. Jensen, Polarization consistent basis sets. III. The importance of diffuse functions, J. Chem. Phys. 117 (2002) 9234–9240.
[17] H.T. Nguyen, V.T.T. Huong, M.T. Nguyen, Silole-based oligomers as electron transport materials, Chem. Phys. Lett 550 (2012) 33–40.
[18] H. Murata, G.G. Malliaras, M. Uchida, Y. Shen, Z.H. Kafafi, Non-dispersive and air-stable electron transport in an amorphous organic semiconductor, Chem. Phys. Lett. 339 (2001) 161–166.
[19] B.Z. Tang, X. Zhan, G. Yu, P.P.S. Lee, Y. Liu, D. Zhu, Efficient blue emission from siloles, J. Mater. Chem. 11 (2001) 2974–2978.
[20] J. Chen, C.C.W. Law, J.W.Y. Lam, Y. Dong, S.M.F. Lo, I.D. Williams, D. Zhu, B. Z. Tang, Synthesis, Light Emission, Nanoaggregation, and Restricted Intramolecular Rotation of 1,1-Substituted 2,3,4,5-Tetraphenylsiloles, Chem. Mater 15 (2003) 1535–1546.
[21] J. Luo, Z. Xie, J. Lam, L. Cheng, H. Chen, C. Qiu, H.S. Kwok, X. Zhan, Y. Liu, D. Zhu, B.Z. Tang, Aggregation-induced emission of 1-methyl-1,2,3,4,5-pentaphenylsilole, Chem. Commun. (2001) 1740–1741.
[22] Y. Shirota, H. Kageyama, Charge Carrier Transporting Molecular Materials and Their Applications in Devices, Chem. Rev. 107 (2007) 953–1010.
[23] L. Aubouy, P. Gerbier, C. Guérin, N. Huby, L. Hirsch, L. Vignau, Study of the influence of the molecular organization on single-layer OLEDs' performances, Synth. Met. 157 (2007) 91–97.
[24] C. Risko, E. Zojer, P. Brocorens, S.R. Marder, J.L. Brédas, Bis-aryl substituted dioxaborines as electron-transport materials: a comparative density functional theory investigation with oxadiazoles and siloles, Chem. Phys. 313 (2005) 151–157.
[25] J. Kunai, J. Ohshita, T. Iida, K. Kanehara, A. Adachi, K. Okita, Synthesis and Properties of Silicon-Bridged Bithiophenes and Application to EL Devices, Synth. Met. 137 (2003) 1007–1008.
[26] J. Mei, J. Wang, J.Z. Sun, H. Zhao, W. Yuan, C. Deng, S. Chen, H. Sung, P. Lu, A. Qin, H.S. Kwok, Y. Ma, I.D. Williams, B.Z. Tang, Siloles symmetrically substituted on their 2,5-positions with electronaccepting and donating moieties: facile synthesis, aggregation-enhanced emission, solvatochromism, and device application, Chem. Sci. 3 (2012) 549–559.
[27] M.M.A.R. Moustafa, B.L. Pagenkopf, Silole based acetylenes as advanced π-conjugated systems for optoelectronic applications, C. R. Chim. 12 (2009) 359–365.
[28] D. Delaere, N.N. Pham-Tran, M.T. Nguyen, Remarkable influence of fluorine substitution on electronic and thermochemical properties of phospholes, Chem. Phys. Lett 383 (2004) 138–142.
[29] D. Delaere, M.T. Nguyen, L.G. Vanquickenborne, Structure−Property Relationships in Phosphole-Containing π-Conjugated Systems: A Quantum Chemical Study, J. Phys. Chem. A 107 (2003) 838–846.
[30] T. Hasegawa, M. Ashizawa, S. Kawauchi, H. Masunaga, N. Ohta, H. Matsumoto, Fluorination and chlorination effects on quinoxalineimides as an electron-deficient building block for n-channel organic semiconductors, RSC Adv. 9 (2019) 10807–10813.
[31] K. Feng, X. Zhang, Z. Wu, Y. Shi, M. Su, K. Yang, Y. Wang, H. Sun, J. Min, Y. Zhang, X. Cheng, H.Y. Woo, X. Guo, Fluorine-Substituted Dithienylbenzodiimide-Based n-Type Polymer Semiconductors for Organic Thin-Film Transistors, ACS Appl. Mater. Inter 11 (2019) 35924–35934.
[32] S. Paek, N. Cho, K. Song, M. Jun, J. Lee, J. Ko, Efficient Organic Semiconductors Containing Fluorine-Substituted Benzothiadiazole for Solution-Processed Small Molecule Organic Solar Cells, J. Phys. Chem. C 116 (2012) 23205–23213.
[33] L. Benatto, M. Koehler, Effects of Fluorination on Exciton Binding Energy and Charge Transport of πConjugated Donor Polymers and the ITIC Molecular Acceptor: A Theoretical Study, J. Phys. Chem. C 123 (2019) 6395–6406.
[34] B. Maiti, A. Schubert, S. Sarkar, S. Bhandari, K. Wang, Z. Li, E. Geva, R.J. Twieg, B. Dunietz, Enhancing charge mobilities in organic semiconductors by selective fluorination: a design approach based on a quantum mechanical perspective, Chem. Sci. 8 (2017) 6947–6953.
[35] M. Facchetti, M.H. Yoon, C.L. Stern, H.E. Katz, T.J. Marks, Building blocks for n-type organic electronics: regiochemically modulated inversion of majority carrier sign in perfluoroarene-modified polythiophene semiconductors, Angew. Chem. 115 (2003) 4030–4033. Angew. Chem. Int. Ed. 42 (2003) 3900-3903.
[36] C.A. Reed, R.D. Bolskar, Discrete Fulleride Anions and Fullerenium Cations, Chem. Rev. 100 (2000) 1075–1120.
[37] M.I. Bruce, Reactions of polycyano-alkenes with alkynyl- and poly-ynyl-Group 8 metal complexes, J. Organomet. Chem. 730 (2013) 3–19.
[38] C.M. Beck, J. Burdeniuc, R.H. Crabtree, A.L. Rheingold, G.P. Yap, A ferrocene-perfluoroarene molecular complex, Inorg. Chem. Acta 270 (1998) 559–562.
[39] M.J. Frisch, et al., Gaussian 09 (version A.02), Gaussian, Inc., Wallingford CT, 2016.
[40] C.G. Zhan, J.A. Nichols, D.A. Dixon, Ionization Potential, Electron Affinity, Electronegativity, Hardness, and Electron Excitation Energy: Molecular Properties from Density Functional Theory Orbital Energies, J. Phys. Chem. A 107 (2003) 4184–4195.
[41] D.J. Tozer, F.D. Proft, Computation of the Hardness and the Problem of Negative Electron Affinities in Density Functional Theory, J. Phys. Chem. A 109 (2005) 8923–8929.
[42] R.G. Parr, R.G. Pearson, Absolute Hardness: Companion Parameter to Absolute Electronegativity, J. Am. Chem. Soc. 105 (1983) 7512.
[43] F.G. Bordwell, J.-P. Cheng, A.V. Satish, C.L. Twyman, Acidities and Homolytic Bond Dissociation Energies (BDEs) of Benzyl-Type C-H Bonds in Sterically Congested Substrates, J. Org. Chem. 57 (1992) 6542–6546.
[44] E. Runge, E.K.U. Gross, Density-Functional Theory for Time-Dependent Systems, Phys. Rev. Lett. 52 (1984) 997–1000.
[45] P. Hohenberg, W. Kohn, Inhomogeneous electron gas, Phys. Rev. 136 (1964) 864–871.
[46] E.K.U. Gross, R.M. Dreizler, Density Functional Theory, Plenum Press, New York, 1995.
[47] R.E. Stratmann, G.E. Scuseria, M.J. Frisch, An efficient implementation of time-dependent density-functional theory for the calculation of excitation energies of large molecules, J. Chem. Phys. 109 (1998) 8218–8224.
[48] Y. Luo, Comprehensive Handbook of Chemical Bond Energies, Taylor & Francis Group, CRC Press, US, 2007.
[49] E. Steiner, P.W. Fowler, Ring Currents in Aromatic Hydrocarbons, Int. J. Quantum Chem. 60 (1996) 609–616.
[50] D. Geuenich, K. Hess, F. Köhler, R. Herges, Anisotropy of the Induced Current Density (ACID), a General Method to Quantify and Visualize Electronic Delocalization, Chem. Rev. 105 (2005) 3758–3772.
[51] D.A. Dixon, D.A. Kleier, W.N. Lipscomb, Localized Molecular Orbitals for Polyatomic Molecules. 6. Condensed Aromatic Ring Systems, J. Am. Chem. Soc. 100 (1978) 5681–5694.
[52] Y.H. Cheng, X. Zhao, K.S. Song, L. Liu, Q.X. Guo, Remote Substituent Effects on Bond Dissociation Energies of Para-Substituted Aromatic Silanes, J. Org. Chem. 67 (2002) 6638–6645.